Augmented Reality Enhanced Image-Guided Surgery System Using CT and Ultrasound Registration for Brain-Shift Estimation

Wei-Chic Huang[1], Chung-Hung Hsieh[1], Chung-Hsien Huang[1], Shin-Tseng Lee[2] , Chieh-Tsai Wu[2]

Yung-Nien Sun[3], Yu-Te Wu[4] and Jiann-Der Lee[1]*

[1]Department of Electrical Engineering, Chang Gung University, Tao-Yuan, Taiwan
[2]Deptartment of Neurosurgery, Chang Gung Memorial Hospital, Tao-Yuan, Taiwan
[3]Department of Computer Science and Information Engineering, National Cheng Kung University,Tainan, Taiwan
[4]Department of Biomedical Imaging and Radiological Sciences, National Yang-Ming University, Taipei, Taiwan

ABSTRACT

In neurosurgery, brain shift, usually caused by the gravity or the changes of intra-cranial pressure, is the main factor to affect the accuracy of tumor removal. To deal with this problem, an image-guided surgery system which corrects the brain shift from the pre-operative CT images by using intra-operative ultrasound images is presented. First, with reconstructing 2-D free-hand ultrasound images to 3-D volume data, the system applies a Mutual-Information based registration algorithm to estimate the deformation between pre-operative and intra-operative ultrasound images. The estimated deformation transform describes the shifts of soft tissues and is then applied to the pre-operative CT images. The brain-shift correction procedure was validated with a brain phantom. When the shift of an artificial tumor is from 5mm ~ 12mm, the overlapping rates can be improved from 32% ~ 45% to 87% ~ 95%. In addition, the system displays the fusion of the corrected CT images or the real-time 2-D ultrasound images with the patient in the physical space through a head mounted display device, providing an immersive augmented-reality environment.

KEYWORDS: Augmented Reality; Image-Guided Surgery; Brain-Shift Estimation; Medical Image Registration

1. INTRODUCTION

Nowadays, image-guided surgery (IGS) has become an important part for neurosurgery. The anatomical information observed from pre-operative medical images such as Computed Tomography (CT) or Magnetic Resonance Imaging (MRI) helps neurosurgeons to diagnosis the status of disease, locate tumor and plan a surgery. With the assistance of IGS, each voxel on the pre-operative images can be linked to a 3-D position in the physical space and be reached by surgical tools, improving the accuracy of target localization and reducing surgical time.

However, pre-operative medical images only provide the information of the patient before surgery but not the up-to-date one. Some surgical targets such as soft tissues may be shifted during the surgery. The shift usually causes inaccurate target localization of IGS system. A simple and ordinary method to solve this problem is using intra-operative CT or MRI; however, this procedure would interrupt the process of operation and may not be practical due to the environmental limitation in operating room. Recently, a significant body of work appears on using intra-operative ultrasound scanner to obtain real-time images, especially on brain surgery [1], cardiac surgery [2], lung surgery

[3], or liver surgery [4]. Since ultrasonic imaging is less damaging than CT and MRI and low cost, intra-operative ultrasound can conveniently be applied during operation. For example, the ultrasound images acquired before and during surgery can be compared with each other in order to estimate the brain shift. The transformation estimated can be further applied to the pre-operative CT or MRI, which provides better and detailed anatomical information. This process helps neurosurgeon to map pre-operative information onto intra-operative situation efficiently.

In the last two decades, Augmented Reality (AR) has been drawn much attention and been adopted in various fields such as education, entertainment, and medical applications. AR could provide surgeons a mapping visualization instead looking away from a patient to consult a manual operation. The study in [5] may be referred as the pioneer of applying AR in the operating room. In [6], a research group at UNC Chapel Hill presented an AR system for ultrasound-guided needle biopsy of breast. In this study, an AR enhanced IGS system using ultrasound and CT registration for brain shift estimation is presented. In the setup of the IGS system, a spatial digitizing device is attached to the probe to obtain the spatial location and orientation of the ultrasound probe. After performing the calibration between the digitizing device and the ultrasound probe, 3-D ultrasound volume data can be reconstructed by using a pixel-based interpolation algorithm. When a patient lies down on the operation table, the coordinate of the patient in the physical space, the preoperative CT of the patient, and of the ultrasound images can thus be integrated into a unified coordinate system. When the brain shift occurs during surgery, the patient is scanned again by the ultrasound scanner. The intra-operative ultrasound images are then utilized to register with the per-operative ultrasound images for the estimation of deformation, which is subsequently applied to update the pre-operative CT, producing better anatomical information and closer to the intra-operative situation.

To validate the performance of the procedure of the brain-shift correction, a brain phantom made by silicone was utilized for testing and evaluation. We simulated the spatial shift with 5mm, 8mm and 12mm by squeezing the brain phantom. The estimated transformation was applied on the pre-operative CT images and the transformed images were compared with ground-truth intra-operative CT images.

Moreover, in general IGS system, the anatomical information resolved from images is usually displayed on the screen. In the proposed system, the medical images are augmented with the patient on the real scene by using an AR head-mounted display (HMD)[7]. The AR display provides more immediate and direct visual experience to neurosurgeons. In addition, the visual display modes can be changed under requirements.

The paper is organized as follows. Section 2 describes the proposed system in detail. Section 3 reveals our experimental

Chang-Gung University, 259 Wen-Hwa 1st Road, Kwei-Shan Tao-Yuan, Taiwan, 333, R.O.C., *corresponding author:jdlee@mail.cgu.edu.tw

results and AR visualization. Conclusions are drawn in Section 4.

2. METHODS

System and Flowchart

Figure 1 shows the presented AR-enhanced IGS system includes image modalities, hardware devices, and their spatial relationships. The following components are involved: preoperative CT images, a portable ultrasound scanner, a digitizing device, a movable camera embedded with an HMD, and a designed black-and-white pattern for AR visualization.

For the IGS installation, firstly, the digitizing device is attached to the ultrasound probe. A commercial digitizing system, NDI Polaris Vicra System [8], abbreviated as NDI hereafter, is adopted as the digitizing device. The coordinates of the NDI (C_{NDI}) and the ultrasound probe (C_{US}) are calibrated with a calibration box, as shown in Fig. 2 (a). Therefore, real-time spatial tracking of the ultrasound probe can be achieved. In addition, the coordinate of the AR pattern (C_{AR}) is also calibrated with the NDI system. When the AR pattern appears in the field of view of the moving camera CAM, the extrinsic parameters of the camera can be estimated through the observed shape of the pattern. As a result, the AR-enhanced visual display can be provided.
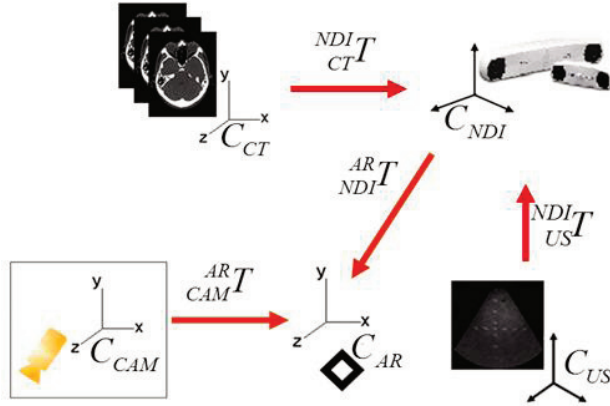
Figure 1. Components involved and their spatial relationships

(a)   (b)
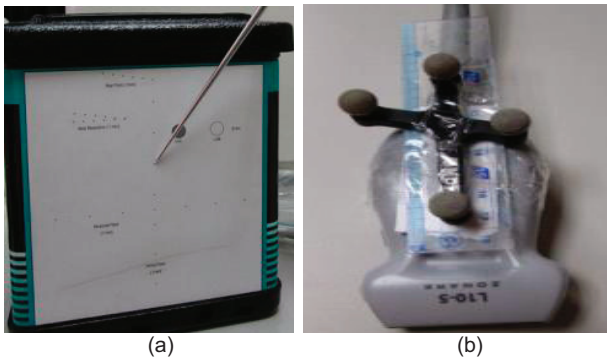
Figure 2. (a) Calibration box for ultrasound/DRF/NDI calibration; (b) Ultrasound probe attached with DRF

Figure 3 shows the flowchart of the medical image registration and AR visualization of the proposed system. Two types of medical imaging modalities are involved: one is ultrasound and the other is per-operative CT (Pre-CT). The ultrasound provides real-time but noisy and low-resolution pre-operative (Pre-US) and intra-operative (I-US) images, while the Pre-CT provides high-

resolution but pre-operative anatomical information. Notably, the soft tissues such as brain observed from the Pre-CT may have some spatial shifts due to the surgical operation or gravity during surgery. In this study, to compensate the shifts we update the Pre-CT via the transformation which was estimated by registering the Pre-CT/Pre-US with Pre-US/I-US images.
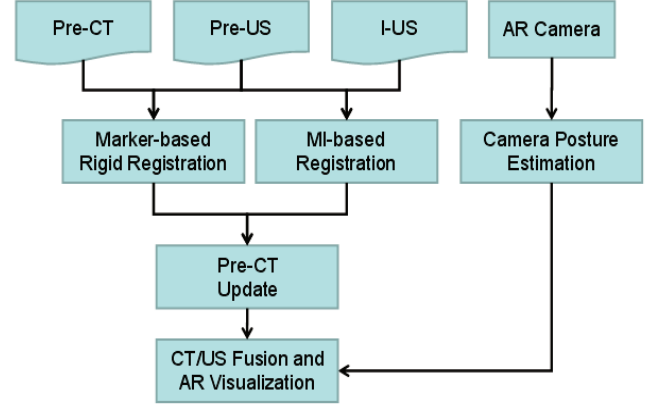
Figure 3. Flowchart of the proposed system for data fusion AR visualization

2.1 Ultrasound/NDI Calibration

In order to map the pixels on the ultrasound image to the physical space, as reported in [9], the ultrasound probe is attached to a trackable device named Dynamic Reference Frame (DRF) of the NDI digitizing system, as shown in Fig. 2 (b). With ultrasound/DRF/NDI calibration, each pixel (x_{US},y_{US}) at the C_{US} can be mapped to a real 3-D location (x_{NDI},y_{NDI},z_{NDI}) of C_{NDI} by applying a 4×4 transform $^{NDI}_{US}T$, which is defined in Eq. (1). The $^{NDI}_{US}T$ is a composition of two transforms $^{NDI}_{DRF}T$ and $^{DRF}_{US}T$, *i.e.*, $^{NDI}_{US}T = {}^{NDI}_{DRF}T \cdot {}^{DRF}_{US}T$, where $^{NDI}_{DRF}T$ is the DRF posture, which can be read directly from the NDI system. The $^{DRF}_{US}T$ is estimated by using least squares method (LSM) [10] with sixteen co-selected points from a calibration box, as shown in Fig. 3(b), by using the NDI digitizer and selecting the corresponding pixels on the ultrasound image. Readers are referred to [2] for the details of the calibration process.

$$\begin{bmatrix} x_{NDI} \\ y_{NDI} \\ z_{NDI} \\ 1 \end{bmatrix} = {}^{NDI}_{US}T \begin{bmatrix} x_{US} \\ y_{US} \\ 0 \\ 1 \end{bmatrix} \tag{1}$$

2.2 3-D Reconstruction of Ultrasound Images

Since the ultrasound scanner provides only 2-D images, a 3-D reconstruction algorithm is applied on a sequence of free-hand 2-D scans to obtain 3-D volume data. In this study, the freehand 3-D ultrasound reconstruction algorithm using Pixel-Based Methods (PBM) proposed by Solberg et al. [11] is employed. The PBM applies a 3-D Gaussian kernel around a voxel, and drives the impact of the voxel to its neighbor voxels as a weighting function. Therefore, the voxel needed to be interpolated can be reconstructed according to the weighted contribution from its neighbors.

2.3 Pre-CT/Pre-US Registration

The Pre-CT/Pre-US registration is accomplished by selecting N landmarks, denoted as P_{NDI}, on the patient by NDI and their corresponding pixels, denoted as P_{CT}, on the CT images. The landmarks could be any artificial skin markers glued externally to the patient or natural feature points of the patient. Therefore, the transform $^{NDI}_{CT}T$ can be calculated by Eq. (2) with LSM if we have at least four landmarks.

$$P_{NDI} = {}^{NDI}_{CT}T \cdot P_{CT} \qquad (2)$$

2.4 Pre-US/I-US Registration and Pre-CT Update

To estimate brain shifts, inspired by the work proposed by Letteboer [1], we estimate a free-form deformation (FFD) transformation by using a nonlinear Pre-US/I-US registration and then update the Pre-CT by the estimated transformation. The basic idea of FFD involves manipulating an underlying mesh of a set of control points to obtain the prostate deformation model. In this study, B-Spline Mutual Information (MI) based algorithm [12] is applied for the task of the nonlinear Pre-US/I-US registration.

B-Spline is a free-form deformation and its basic idea is locating an object within a mesh so that the object deforms according to the deformation of the mesh. B-Spline registration manipulates the mesh via a set of control points and naturally lends itself for multi-resolution registration.

MI is defined to maximize the common information shared by the two images to be registered and to reduce the information in the combined image. The more correlated the two images, the lower joint entropy. The implementation of the B-Spline MI-based algorithm is accomplished by using the Insight Segmentation and Registration Toolkit library (ITK) [13] and can be simply expressed by the following equation.

$$\widehat{T} = \arg\max_{T_{\text{B-Spline}}} MI(\text{Pre-US}, \text{I-US}, T_{\text{B-Spline}}) \qquad (3)$$

Through the step of the Pre-US/I-US registration, the non-rigid brain shifts could thus be compensated, *i.e.*, using the non-linear transformation estimated by the B-Spline MI-based algorithm. The estimated transformation can then be applied to the Pre-CT, obtaining the intra-operative CT (I-CT'), *i.e.*, I-CT' = $\widehat{T}$(Pre-CT).

2.5 AR Visualization

After performing the mentioned image-to-patient (section 2.4) and image-to-image (section 2.5) registrations, the Pre-CT and I-US are integrated to the physical space of the patient, *i.e.*, the NDI coordinate system. With the use of ARTOOLKIT [14], an HMD device attached with a CCD camera is applied to provide an immersive AR environment for uses. The pose of the camera can be estimated through observing a designed black-and-white AR pattern. Note that the AR pattern should be calibrated with the NDI coordinate system before surgery. The calibration procedure is accomplished by selecting the four corners around the AR pattern by NDI, and the estimating the transform $^{AR}_{NDI}T$ by LSM as well. Figure 4 (a) shows the HMD and the camera, and Fig. 4 (b) is the AR pattern. The adopted HMD is Iwear-VR920 made by VUZIX Inc [15].

3. RESULTS

A phantom made by silicone was utilized to validate the procedure of the brain-shift correction. The shape of the phantom was reconstructed according to a brain 3-D model segmented from a set of MRI images. In addition, a balloon filled with glycerin was attached beneath the brain surface as a simulation of brain tumor. Figure 5 (a) and (b) show the phantom and its 3-D reconstruction model, respectively. The phantom was placed within a plastic cubic and performed CT scan four times. The first scan was under normal situation, while in the other scans the surface of phantom was squeezed with a plastic rod to simulate the effect causing by brain shifts, as shown in Fig 5(c), (d), and (e), where the red circles indicate the location of the glycerin balloon. The first scan was regarded as the Pre-CT, and the others were regarded as intra-operative CT (I-CT) and denoted as Scan-A, Scan-B and Scan-C. We estimated the overall shift of the glycerin balloon by measuring the distance between its gravity centers calculated in Pre-CT and I-CTs. The overall shifts of Scan-A, Scan-B and Scan-C are 5mm, 8mm, and 12mm, respectively. The volume size of CT image is $512 \times 512 \times 324$ and the voxel size is $0.4 \times 0.4 \times 0.8$ mm^3, while the volume size of US image is 230×350 and the pixel size is 0.6×0.6 mm^2. The ultrasound device is made by ZONARE Medical Systems Inc.

Figure 4. Components for AR visualization (a) HMD and the camera attached; (b) AR pattern

3.1 Evaluation on Image Registration

Figure 6 illustrates an instance of the CT/US registration results with Scan-A. In Fig.6 (a), the Pre-US and Pre-CT are shown by gray scale and green, respectively. For better visualization, the contour of the glycerin balloon was extracted manually from the Pre-CT and laid on the Pre-US, as shown in Fig. 6 (d). Similarly, Fig. 6(b) and (e) show the fusion results of the Pre-CT and I-US. The shift of the glycerin balloon caused by squeezing brain can be observed easily from the fusion images. The B-Spline MI-based registration was applied on Pre-US and I-US, resulting in a nonlinear transform $\widehat{T}$, as defined in Eq. (3). The transform was utilized to update the Pre-CT so that it can be deformed based on the estimated brain shifts and denoted as I-CT'. The results of I-US/I-CT' fusion are shown in Fig. 6 (c) and (f) where the I-CT' is colored in blue.

Since the CT scans of the phantom with different deformations were performed, they could be adopted as the ground truth to evaluate the performance of compensating the brain shift. Figure 7 (a) and (b) show the chessboard-like image fusion and the contours of the glycerin balloon, respectively. The green line indicates the contour extracted from the Pre-CT image, while the red line is from the I-CT image, *i.e.*, Scan-A. After updating the Pre-CT by the transform $\widehat{T}$, the shift effect is thus corrected and

illustrated in Fig. 7 (c) and (d). The blue line in Fig. 7(d) indicates the contour of the glycerin balloon extracted from the updated Pre-CT, *i.e.*, I-CT'. It can be seen that the I-CT's provides more accurate anatomical information than Pre-CT.

(a)

(b)

(c)

(d)

(e)
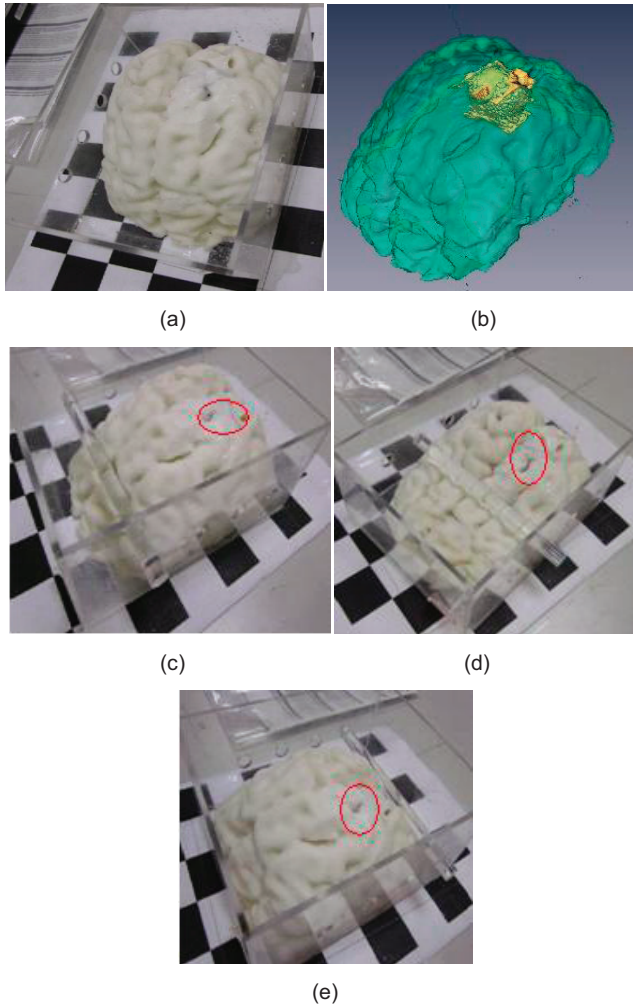
Figure 5. Brain phantom for evaluation (a) the phantom; (b) 3-D model of the phantom; (c), (d) and (e) the phantom squeezed under different pressure.

(a)

(b)

(c)

(d)

(e)

(f)
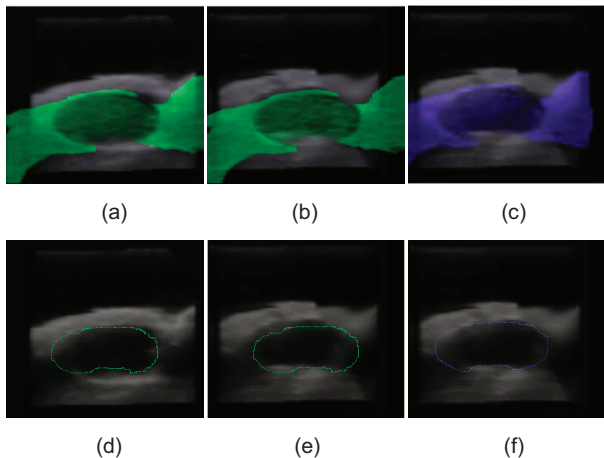
Figure 6. An instance showing the image fusion results of CT/US registration. (a) Pre-CT/Pre-US fusion; (b) Pre-CT/I-US fusion; (c) image fusion of I-US and updated Pre-CT; (d) overlapping the Pre-CT contour on Pre-US; (e) overlapping the Pre-CT contour on I-US; (f) overlapping the updated Pre-CT contour on I-US.

(a)

(b)

(c)

(d)
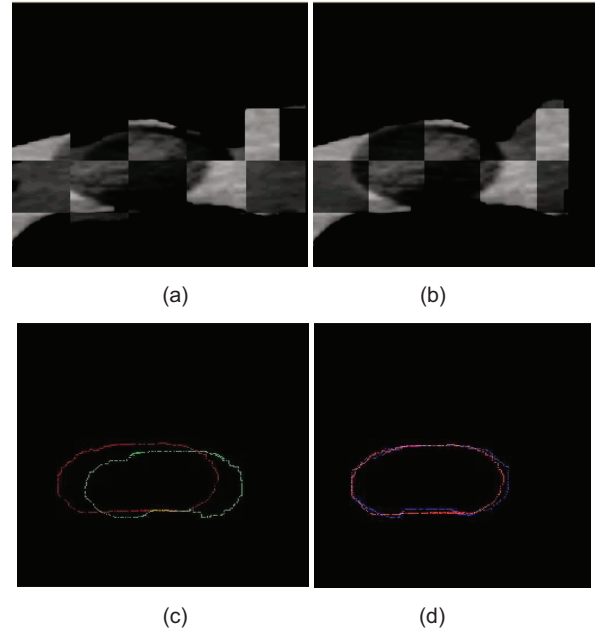
Figure 7. Comparison among Pre-CT, I-CT and I-CT' (a) chessboard-like fusion of Pre-CT and I-CT; (b) chessboard-like fusion of I-CT' and I-CT; (c) contours of the glycerin balloon extracted from Pre-CT (green) and I-CT (red); (d) contours of the glycerin balloon extracted from I-CT' (blue) and I-CT (red)

More precisely, we measure the overlapping rate of the glycerin balloon between the I-CT' and I-CT to validate the performance of brain-shift estimation. The overlapping rate is defined as $(A \cap B)/(A \cup B)$, where A is the volume of the glycerin balloon in the I-CT and B is its volume in the I-CT'. Figure 8 shows the overlapping rate before and after performing brain-shift estimation of the three CT scans. The overlapping rates of Scan-A, Scan-B and Scan-C were 97%, 95%, and 87%, respectively. It is anticipated that the larger is the brain shift, the lower is the compensation accuracy.

	Scan-A	Scan-B	Scan-C
I-CT'	97	94	87
Pre-CT	45	40	32
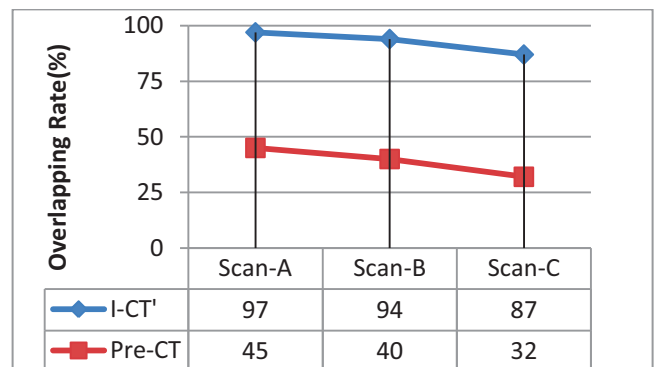
Figure 8. Comparison of brain-shift estimation among Scan-A, Scan-B and Scan-C.

3.2 Augmented Reality Display

Finally, we demonstrate the immersive AR display provided by the proposed system. The AR display mode is switchable according to the user's need. The available modes include displaying the reconstructed CT 3-D model, the real-time ultrasound image, or a mixture of them. Figure 9 (a) shows the fusion of the phantom and the I-CT', Fig.9 (b) is with the I-US, and Fig. 9 (c) shows the glycerin balloon extracted from I-CT' with I-US.

(a)

(b)

(c)
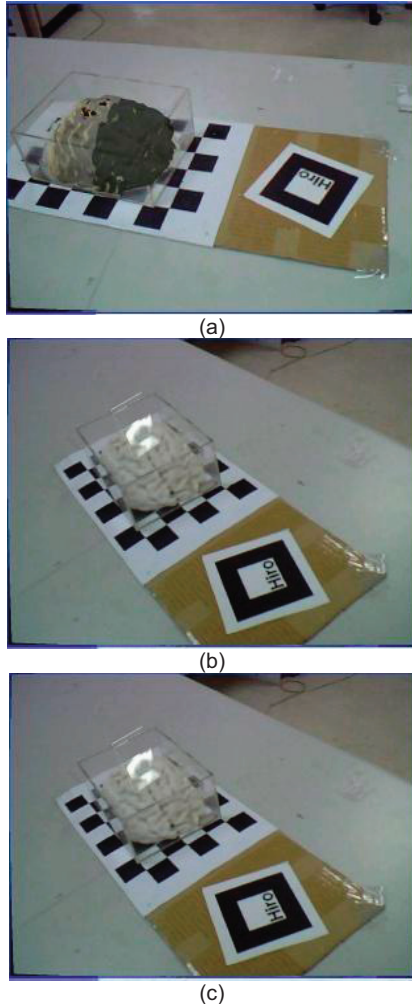
Figure 9. Results of AR display (a) augmented with I-CT'; (b) augmented with I-US; (c) augmented with a mixture of I-CT' and I-US.

4. CONCLUSION

In this study, we have presented an AR-enhanced IGS system using preoperative CT and intra-operative ultrasound. The preoperative CT provides anatomical information of patient, the intra-operative ultrasound produces real-time images during the surgery, and the AR display provides user a direct and integrated visualization experience.

Furthermore, the application of proposed system to the brain surgery application for brain-shift estimation was also investigated. In order to estimate the brain shift, a non-rigid image registration method based on Mutual Information and free-form B-spline deformation was adopted. The registration method was applied to estimate the deformation between pre-US and I-US, and then update pre-CT by the estimated transformation. Thus the updated pre-CT showed better representation on the current situation of the patient than the pre-CT.

So far, the experiments for validating the proposed system are only performed on phantoms, future works will test the system on animal trials. In addition, the brain-shift estimation model can be further connected with a brain biomechanical model for a more realistic estimation.

REFERENCES

[1] M. M. Letteboer, P. W. Willems, and W. J. Niessen, "Brain Shift Estimation in Image-Guided Neurosurgery Using 3-D Ultrasound," IEEE Transactions on Biomedical Engineering, vol. 52, no. 2, pp. 268-286, 2005

[2] X. Huang, J. Ren, G. Guiraudon, D. Boughner, and T. M. Peters, "Rapid Dynamic Image Registration of the Beating Heart for Diagnosis and Surgical Navigation," IEEE Transactions on Medical Imaging, vol. 28, pp. 1802-1814, 2009

[3] N. A. Sadeghi, R. V. Patel, and A. Samani, "CT-Enhanced Ultrasound Image of a Totally Deflated Lung for Image-Guided Minimally Invasive Tumor Ablative Procedures," IEEE Transactions on Medical Imaging, vol. 57, no. 10, pp. 2627-2630, 2010

[4] W. Wein, O. Kutter, A. Aichert, D. Zikic, A. Kamen, and N. Navab, "Automatic Non-Linear Mapping of Pre-procedure CT Volumes to 3D Ultrasound," In Proceedings of the 2010 IEEE international conference on Biomedical imaging: from nano to Macro, pp. 1225-1228, 2010

[5] W. Lorensen, H. Cline, C. Nafis, R. Kikinis, D. Altobelli and L. Gleason, "Enhancing Reality in the Operating Room," in Proceedings of Visualization'93, pp. 410-415, 1993.

[6] A. State, M. A. Livingston, W. F. Garrett, G. Hirota, M. C. Whitton, E. D. Pisano and H. Fuchs, "Technologies for Augmented Reality Systems: Realizing Ultrasound Guided Needle Biopsies," in Proceedings of SIGGRAPH'96, vol. 30, pp. 439-446, 1996.

[7] T. Blum, S. M. Heining, O. Kutter, and N. Navab, "Advanced Training Methods Using Augmented Reality Ultrasound Simulator," In Proceedings of IEEE International Symposium on Mixed and Augmented Reality, pp. 19-22, 2009

[8] Northern Digital Inc., http://www.ndidigital.com/

[9] H. Zhang, F. Banovac, K. Cleary, and A. White, "Freehand 3D Ultrasound Calibration Using an Electromagnetically Tracked Needle," In Proceedings of the SPIE, vol. 6141, pp. 775-783, 2007

[10] W. M. Donald, "An Algorithm for Least-Squares Estimation of Nonlinear Parameters," Journal of the Society for Industrial and Applied Mathematics, pp. 431-441, 1963

[11] O. V. Solberg, F. Lindseth, H. Torp, R. E. Blake, and T. A. Hernes, "Freehand 3D Ultrasound Reconstruction Algorithms - A Review," Ultrasound in Med & Biol, vol. 33, no. 7, pp. 991-1009, 2007

[12] Y. Jin and G. Ma, "Investigation and Evaluation of Optimal Registration for Medical CT Images," International Congress on Image and Signal Processing, pp. 2794-2797, 2010

[13] Insight Segmentation and Registration Toolkit., http://www.itk.org/

[14] Artoolkit 2002, http://www.washington.edu/ARTOOLKIT/

[15] Vuzix Inc., http://www.vuzix.com/home/